AGU PUBLICATIONS

Geophysical Research Letters

RESEARCH LETTER
10.1002/2015GL064764

Key Points:
- Greenland temperatures over the past 2100 years were reconstructed
- Late twentieth century cooling in Greenland was due to modern solar maximum
- Spatial temperature responses to solar variation indicate involvement of AMOC

Supporting Information:
- Text S1 and Figures S1–S8
- Tables S1–S5

Correspondence to:
T. Kobashi,
kobashi@climate.unibe.ch

Citation:
Kobashi, T., J. E. Box, B. M. Vinther, K. Goto-Azuma, T. Blunier, J. W. C. White, T. Nakaegawa, and C. S. Andresen (2015), Modern solar maximum forced late twentieth century Greenland cooling, *Geophys. Res. Lett.*, *42*, 5992–5999, doi:10.1002/2015GL064764.

Received 1 JUN 2015
Accepted 23 JUN 2015
Accepted article online 25 JUN 2015
Published online 21 JUL 2015

Modern solar maximum forced late twentieth century Greenland cooling

T. Kobashi[1,2,3], J. E. Box[4], B. M. Vinther[5], K. Goto-Azuma[3,6], T. Blunier[5], J. W. C. White[7], T. Nakaegawa[8], and C. S. Andresen[4]

[1]Climate and Environmental Physics, University of Bern, Bern, Switzerland, [2]Oeschger Centre for Climate Change Research, University of Bern, Bern, Switzerland, [3]National Institute of Polar Research, Tokyo, Japan, [4]Geological Survey of Denmark and Greenland, Copenhagen, Denmark, [5]Center for Ice and Climate, University of Copenhagen, Copenhagen, Denmark, [6]Department of Polar Science, SOKENDAI (The Graduate University for Advanced Studies), Tokyo, Japan, [7]Institute of Arctic and Alpine Research, University of Colorado, Boulder, Colorado, USA, [8]Meteorological Research Institute, Tsukuba, Japan

Abstract The abrupt Northern Hemispheric warming at the end of the twentieth century has been attributed to an enhanced greenhouse effect. Yet Greenland and surrounding subpolar North Atlantic remained anomalously cold in 1970s to early 1990s. Here we reconstructed robust Greenland temperature records (North Greenland Ice Core Project and Greenland Ice Sheet Project 2) over the past 2100 years using argon and nitrogen isotopes in air trapped within ice cores and show that this cold anomaly was part of a recursive pattern of antiphase Greenland temperature responses to solar variability with a possible multidecadal lag. We hypothesize that high solar activity during the modern solar maximum (approximately 1950s–1980s) resulted in a cooling over Greenland and surrounding subpolar North Atlantic through the slowdown of Atlantic Meridional Overturning Circulation with atmospheric feedback processes.

1. Introduction

Over the past two decades, Greenland near-surface air temperatures have increased rapidly [*Box*, 2013], forcing mass loss from the Greenland Ice Sheet [*Hanna et al.*, 2013]. During this period, the ice sheet has contributed approximately one third of the global sea level rise of 3.22 ± 0.41 mm/yr from 1992 to 2011 [*Hanna et al.*, 2013]. However, during the preceding decades (i.e., 1970s to early 1990s), Greenland and the surrounding subpolar North Atlantic experienced anomalously low temperatures amid rising Northern Hemispheric average temperatures (Figure 1) [*Box*, 2013; *Kobashi et al.*, 2011; *Levitus et al.*, 2012]. This cooling and subsequent warming since 1995 is a regional pattern attributed to the Atlantic Multidecadal Oscillation (AMO) [*Häkkinen et al.*, 2011]. Recent studies indicate that temperature changes in the North Atlantic before and after 1995 were induced by changes in the frequency of atmospheric blocking activity and associated changes in warmer and more saline seawater in the subpolar North Atlantic [*Häkkinen et al.*, 2011], and Atlantic Meridional Overturning Circulation (AMOC) likely played an important role for these changes [*Chen and Tung*, 2014; *Polyakov et al.*, 2010; *Rahmstorf et al.*, 2015]. However, the underlying causes of the multidecadal variations remain unknown.

Multidecadal temperature variability is only just captured by observational records of the past 13 decades, and while longer time resolution paleorecords resolve multidecadal and centennial variability, they have larger uncertainties and are biased by seasonality, making it difficult to capture small multidecadal temperature signals. To address this, we have developed a tool to capture multidecadal to centennial surface temperature variations over Greenland with sufficiently high precision in both temperature and age [*Kobashi et al.*, 2011, 2010], using argon and nitrogen isotopes of air trapped in ice cores from the Greenland Ice Sheet. In an unconsolidated snow layer (firn) on an ice sheet, gases fractionate according to the depth of the firn and the temperature gradient between the top and bottom of the layer [*Severinghaus et al.*, 1998]. Measurements of nitrogen and argon isotopic ratios allow us to separate the effects of gravitational enrichment and thermal diffusion and to reconstruct past temperature gradients (ΔT) in the firn layer [*Severinghaus et al.*, 1998]. The ΔT can be integrated to reconstruct robust surface temperature changes in the past (ΔT integration method) to be consistent with borehole temperature profiles using a firn densification/heat diffusion model [*Kobashi et al.*, 2011, 2010]. Importantly, the reconstructed temperature records are physically constrained and seasonally unbiased estimators of multidecadal temperature changes (supporting information).

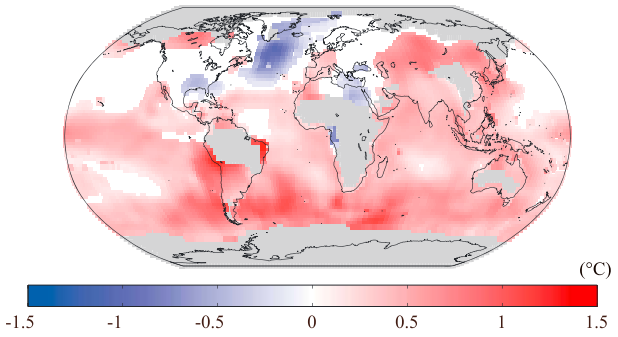

Figure 1. Surface temperature differences for the averages of two periods, i.e., 1920–1940 and 1975–1995 (also see Figure 5). Only grids with 95% confidence intervals are shown. Data are from the GISS Land-Ocean Temperature Index [*Hansen et al.*, 2010]. The grey areas indicate grids with continuous data not available for the entire period.

2. Data

In this study, we present a new Greenland surface temperature record for the past 2100 years using the North Greenland Ice Core Project (NGRIP) ice core. Combined with a temperature reconstruction [*Kobashi et al.*, 2011] from the Greenland Summit (Greenland Ice Sheet Project (GISP) 2; Figure 2 and Figure S1 in the supporting information), we find that NGRIP and GISP2 exhibit coherent multidecadal to centennial variations over the past 1000 years ($r = 0.78$, $P = 0.1$; $r = 0.67$, $P < 0.001$ after linear detrending) with higher sampling densities (Figure S2) than that of the earlier 1100 year period (1000 Common Era (C.E.) to 100 before the Common Era; $r = 0.28$, $P = 0.16$). Comparisons between the reconstructed temperature and isotope records (e.g., δ^{15}N and δ^{40}Ar) exhibit physically consistent relations between changes in temperature and firn thickness over the entire period, which supports the reconstructed temperatures (Figure S3). Surface temperatures were also reconstructed directly from borehole temperature records using two different methods (supporting information) and revealed consistent multicentennial trends with the ΔT integration method within their uncertainties (Figure 2 and Figures S4b and S4c).

To check the methods, we conducted synthetic temperature experiments with an assumption that surface temperature signals of the NGRIP and GISP2 are identical (supporting information). Synthetic surface temperatures for 1900 years (Figure S5), which have similar absolute temperatures and variance with Greenland temperatures based on a Northern Hemispheric (NH) temperature record [*Moberg et al.*, 2005], were used to produce synthetic ΔTs and borehole temperatures using a firn densification/ heat diffusion model [*Goujon et al.*, 2003]. Then, the ΔT time series and borehole temperatures were degraded to produce two time series with the same resolution and uncertainties as the NGRIP and GISP2. Thereafter, the surface temperatures were reconstructed using the same procedure for the ice core data.

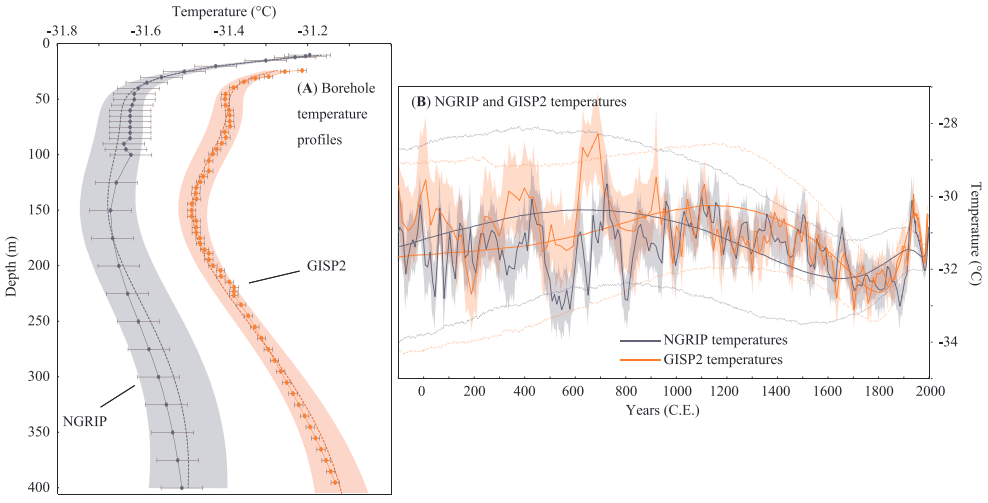

Figure 2. Borehole temperature profiles and reconstructed Greenland temperatures for NGRIP and GISP2. (a) Observed and modeled borehole temperature profiles. Observations are circles with 1σ error bounds (supporting information). The dotted lines are the optimum solutions for the surface temperature reconstruction using the ΔT integration method; the shaded areas represent 95% confidence intervals. (b) Reconstructed Greenland temperatures using the ΔT integration method (with multidecadal variations) and linearized inversions (smooth curbs) based on the NGRIP and GISP2 data. The thick lines are the optimum solutions. The thin lines or shaded areas indicate 95% confidence intervals. All reconstructions including other methods using the borehole temperatures are shown in Figures S4b and S4c.

The two reconstructed synthetic surface temperatures with the ΔT integration method capture the original surface temperature well within their uncertainties ($r = 0.91$, $P < 0.01$ for NGRIP resolution; $r = 0.83$, $P < 0.01$ for GISP2 resolution; Figure S4a). The temperature records with the ΔT integration method show a similar difference in the correlation as the observation in ice cores before and after 1000 C.E. ($r = 0.26$, $P = 0.1$ and $r = 0.91$, $P = 0.14$, respectively; Figure S4a), indicating that the difference in the correlation in the ice core records can be explained by the difference in the sampling density. The synthetic experiments further show that the combined record of the two synthetic temperatures captures multidecadal to centennial surface temperature variability better than the individual records, accounting for up to 77% of the total variance with >99% significance over the entire 1900 years and 25% and 93% of the total variance before and after 1000 C.E., respectively. Therefore, we used the combined record of the NGRIP and GISP2 records (hereafter, Greenland temperature; supporting information) for the following analyses.

3. Results

The reconstructed Greenland temperature over the past 2100 years exhibits common features with the NH temperatures (Figure 3a) [*Hegerl et al*., 2007; *Ljungqvist*, 2010; *Mann et al*., 2008; *Moberg et al*., 2005] such as the Little Ice Age, the Medieval Warm Period, and multidecadal variations but with noticeable differences. Toward the end of the twentieth century, NH temperatures exhibited a steep rise; however, the Greenland temperatures remained anomalously low (Figure 3a). Major drivers of hemispheric climate change over the past millennium are attributable to changes in solar irradiance, volcanism, greenhouse gases, and internal variability [*Crowley*, 2000]. However, regional climate may further deviate from the hemispheric trend owing to regional atmospheric and oceanic circulation changes induced by forcing (e.g., solar activity). For example, stronger (weaker) solar activity produced negative (positive) temperature anomalies from the hemispheric temperature trend in Greenland (Figures 3b and 3c) [*Kobashi et al*., 2013a, 2013b].

To quantify the regional temperature anomalies, multiple linear regressions were applied with NH proxy temperatures [*Hegerl et al*., 2007; *Ljungqvist*, 2010; *Mann et al*., 2008; *Moberg et al*., 2005] and reconstructed total solar irradiance (TSI) [*Roth and Joos*, 2013; *Steinhilber et al*., 2012] as variables, allowing lags for the solar signals (Figure 3c) (supporting information). We used four different NH proxy temperatures [*Hegerl et al*., 2007; *Ljungqvist*, 2010; *Mann et al*., 2008; *Moberg et al*., 2005] and two TSI reconstructions [*Roth and Joos*, 2013; *Steinhilber et al*., 2012] (i.e., eight combinations) to identify the range of the uncertainties (supporting information). The averaged results from the eight combinations were plotted in Figures 3d and 3e, and the coefficients for all the combinations were given in Table S1 in the supporting information. A long-term cooling trend by Earth's orbital change [*Kobashi et al*., 2013a] was determined as a slope of 0.38°C per 1000 years for the past 4000 years of the Greenland temperatures, and it was subtracted from the Greenland temperatures before performing the regression analyses.

The regression models capture the multidecadal Greenland temperature variations ($r = 0.58$, $P = 0.07$ and $r = 0.5$, $P = 0.02$ after linear detrending; Figure 3d; individual results range from $r = 0.65$ to 0.46) with 10 to 40 year lags for the solar signals (Table S1). Consistent with our earlier studies over the past 4000 years [*Kobashi et al*., 2013a, 2013b] that include periods of warmer climate than present, the solar variability is associated with robust antiphase temperature anomalies in Greenland, such that when solar activity increased (decreased), Greenland became colder (warmer) (Figures 3b and 3c). Because the antiphase solar signals in Greenland temperatures persisted over the past 4000 years [*Kobashi et al*., 2013a], the possibility of the influences by volcanic forcing for the antiphase responses can be rejected. The regression analyses suggest that an increase in solar activity from the Maunder Minimum to the Modern Maximum forced Greenland to cool by 1.3 ± 0.1°C (a difference between two periods of 1698–1717 and 1975–1995), cancelling a large part of the hemispheric-wide warming (1.8 ± 0.2°C) with a polar amplification factor of 3.5 ± 0.7 (Figure 3e and Table S1).

To further investigate mechanisms responsible for changes in Greenland temperatures, we conducted the same multiple regressions (NH temperature + solar forcing) on "global grid proxy temperatures" [*Mann et al*., 2009] for 1200–2000 and "Goddard Institute for Space Studies (GISS) global grid surface temperatures" [*Hansen et al*., 2010] for 1890–2003 for multidecadal variations (21 year running means: RMs), allowing lags for the solar forcing (supporting information). The regression with the NH average temperature as a variable removes large anthropogenic warming signals. The results confirm that the antiphase temperature responses

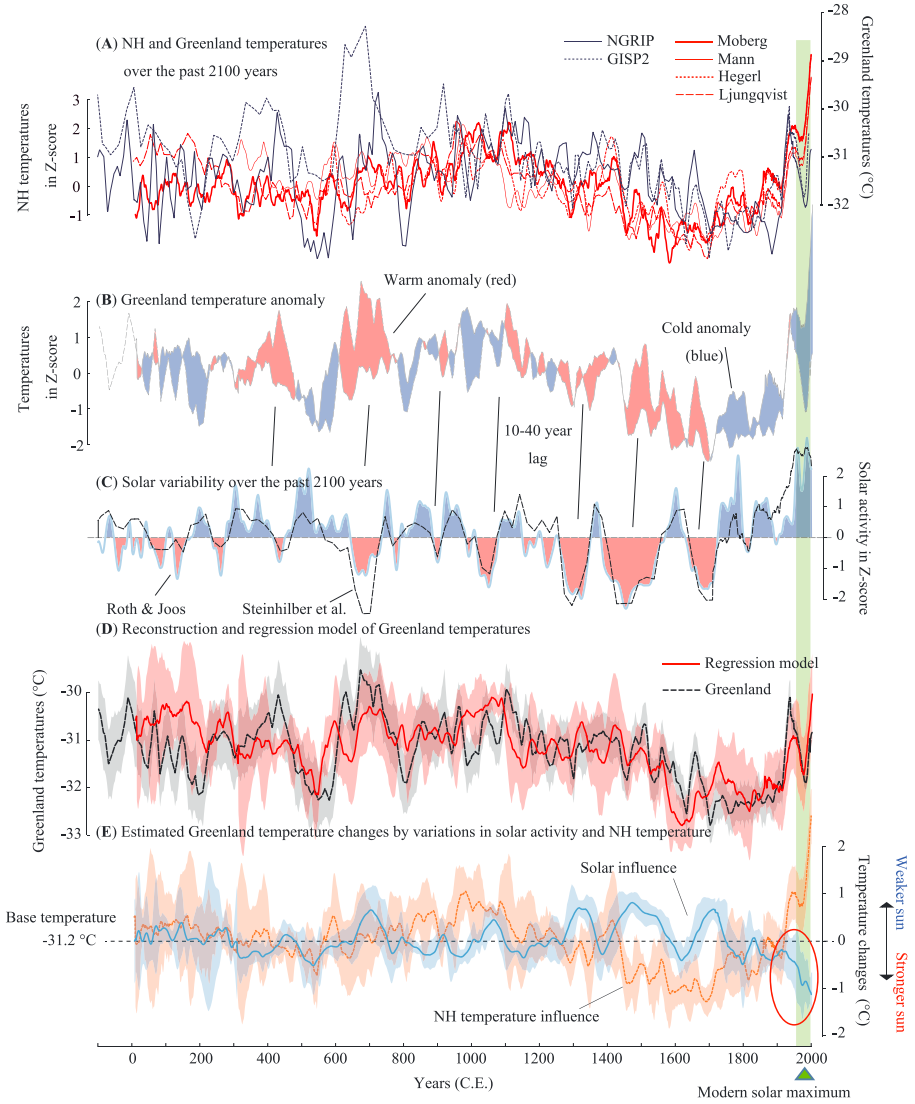

Figure 3. Reconstructed, decomposed, and modeled Greenland temperatures and NH proxy temperatures over the past 2100 years. (a) Reconstructed Greenland temperatures and NH proxy temperatures in *z*-score [*Hegerl et al.*, 2007; *Ljungqvist*, 2010; *Mann et al.*, 2008; *Moberg et al.*, 2005]. These four NH proxy temperatures [*Hegerl et al.*, 2007; *Mann et al.*, 2008; *Moberg et al.*, 2005] were used to calculate average and errors for later analyses (supporting information). (b) Greenland temperature anomaly. Average NH temperature from the four NH records and combined Greenland temperatures were used. Periods of warm (cold) anomalies in Greenland were in red (blue). (c) Two TSI reconstructions by Steinhilber et al. [*Steinhilber et al.*, 2012] and Roth and Joos [*Roth and Joos*, 2013] in *z* score. The blue (red) areas are the periods of stronger (weaker) solar activity corresponding to Figure 3b with possible multidecadal lags. (d) Combined Greenland temperatures (black) and average regression model (red) with the 95% confidence intervals (supporting information). (e) Decomposition of the Greenland temperatures into solar-induced changes (blue) and hemispheric influences (orange) with a regression constant (−31.2°C; dots), constrained by the multiple linear regressions (supporting information). The error bounds are the 95% confidence intervals. The green shaded area is the period (the late twentieth century) when the modern solar maximum had strong negative influence (red circle) on the Greenland temperature.

to solar variability occurred over the subpolar North Atlantic. Maximum surface temperature responses to solar forcing were obtained after a 30 to 40 year lag (Figure 4; see also Figure S6). Similar multidecadal lags have been observed in the analyses of global grid proxy temperatures for preindustrial periods [*Shindell et al.*, 2001; *Waple et al.*, 2002] and an annually dated ice core record from Altai [*Eichler et al.*, 2009]. Two different time frames over the past 801 years and the past 134 years show similar spatiotemporal patterns in the North Atlantic (Figure 4), indicating that this feature is robust in the climate system, operating at least

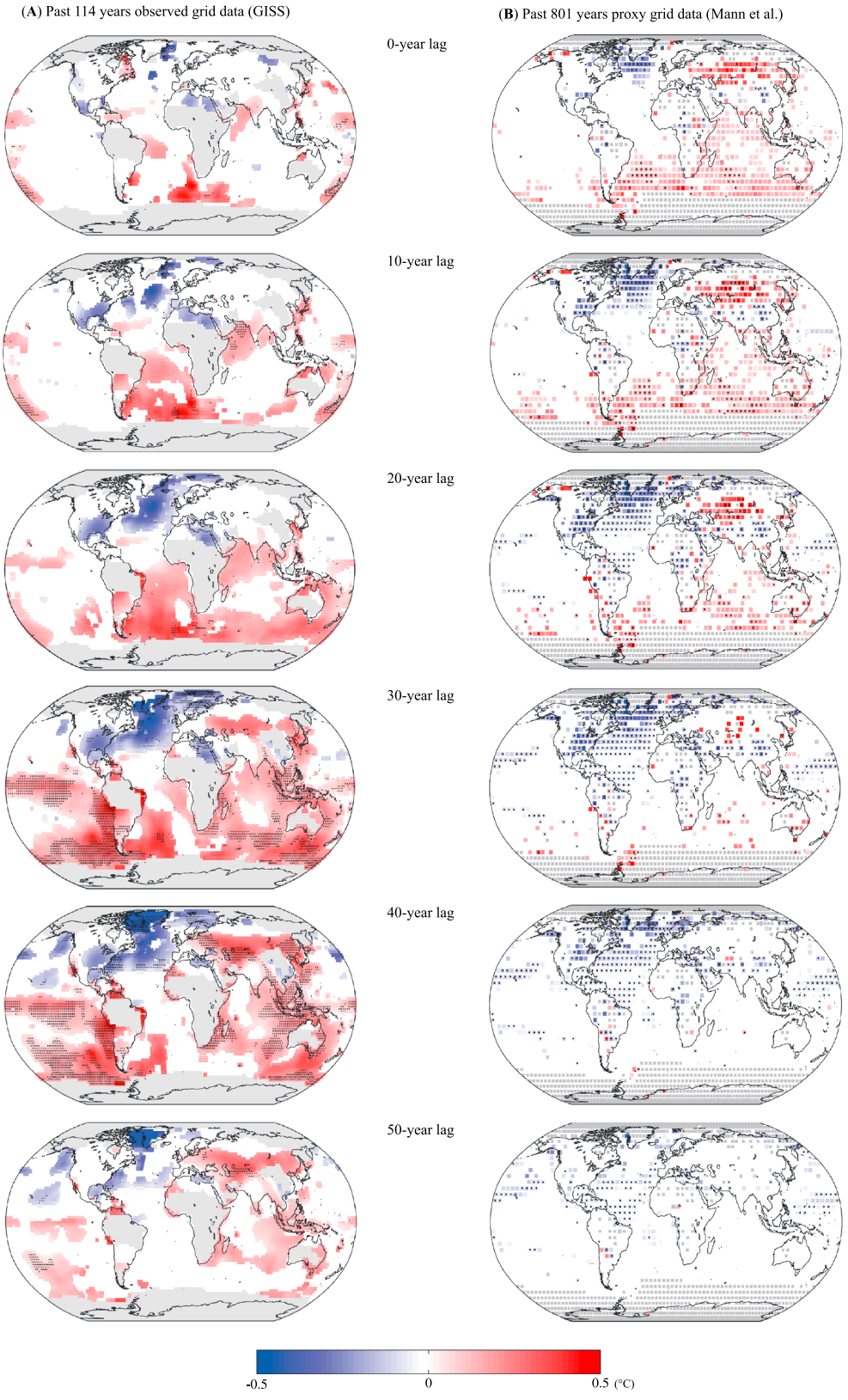
(A) Past 114 years observed grid data (GISS)
(B) Past 801 years proxy grid data (Mann et al.)
0-year lag
10-year lag
20-year lag
30-year lag
40-year lag
50-year lag
-0.5
0
0.5 (°C)

Figure 4

over the past millennium [*Kobashi et al*., 2013a; *Shindell et al*., 2001; *Waple et al*., 2002]. The analyses were repeated with different solar activity reconstructions and global grid temperature data set, and comparable results were found (supporting information).

Similar spatiotemporal temperature changes (e.g., multidecadal lags) in the North Atlantic Basin have been identified in coupled climate model simulations with TSI variations (first mechanism) [*Cubasch et al*., 1997; *Swingedouw et al*., 2011; *Waple et al*., 2002]. In these models, increasing solar activity induces a buoyancy forcing due to warming and increased freshwater inputs into the subpolar North Atlantic, which reduces deepwater formation (or AMOC strength) and lead to a reduction in heat transport from low to high latitudes [*Menary and Scaife*, 2014; *Swingedouw et al*., 2011; *Waple et al*., 2002]. This results in a cooling in the subpolar North Atlantic (i.e., Greenland) and induces a positive North Atlantic Oscillation (NAO)-like atmospheric circulation [*Gastineau and Frankignoul*, 2012; *Swingedouw et al*., 2011]. The negative temperature responses of the subpolar North Atlantic are often reproduced in climate models as a result of increasing atmospheric CO_2 concentration [*Collins et al*., 2013]; however, the effect of increasing CO_2 concentrations alone fails to explain the rapid warming in the subpolar North Atlantic since 1995.

A second mechanism linking solar activity with temperature changes involves stratospheric ozone feedback with solar UV variation [*Gray et al*., 2010; *Kidston et al*., 2015; *Shindell et al*., 2001]. During stronger (weaker) solar activity, stratospheric temperatures increase (decrease) via ozone absorptions of UV sunlight, which increases the temperature gradient between stratospheric high and low latitudes. The change in the meridional temperature gradient leads to strengthened (weakened) westerlies in the midlatitudes, inducing positive (negative) NAO-like conditions in the troposphere. The NAO-like atmospheric response lags the 11 year solar cycle by approximately 3 years, likely owing to the ocean-atmosphere coupling [*Kidston et al*., 2015; *Scaife et al*., 2013].

The observed multidecadal lag with the basin-wide cooling signal suggests that the first mechanism, involving a large-ocean heat reservoir, played a major role in setting the centennial to multidecadal solar signals on surface temperature variability in the subpolar North Atlantic.

Observational data over the past 160 years provide important clues to the multidecadal solar influence on the North Atlantic region. Figures 5a and 5c show the reconstructed and observed Greenland temperatures and the regression models that are constrained over the past 2000 years. The Greenland cooling in the late twentieth century corresponds to the time when the modern solar maximum (a period around 1950s-1980s of high solar activity compared with that of the past millennia) [*Roth and Joos*, 2013; *Steinhilber et al*., 2012] is expected to have maximum cooling effects in Greenland (-0.6 ± 0.1°C: a difference of the average temperatures between 1920–1940 and 1975–1995; Figure 5b). The cooling contrasts a hemispheric warming signal with the polar amplification (0.8 ± 0.1°C) over the same period (Figure 5b). The spatial characteristics of the cold anomalies in 1975–1995 relative to the warm anomalies in 1920–1940 resemble multidecadal solar signals in the North Atlantic (compare Figure 1 with Figure 4). Indeed, decadal solar signals [*Ball et al*., 2012; *Krivova et al*., 2010] with a 34 year lag are significantly correlated ($r = 0.75$, $P = 0.02$ after linear detrending) with the first principal component (PC1) of the wind stress curl in the North Atlantic (Figure 5d), which is an important parameter for the ocean-atmosphere coupling and closely associated with the NAO and Greenland blocking [*Häkkinen et al*., 2011].

Surface temperatures and hydrographic data for the North Atlantic and climate models indicate that the AMOC likely weakened from the middle to the late twentieth century and has strengthened since approximately 1995

Figure 4. Spatiotemporal pattern of the solar influence on global grid surface temperatures in a multidecadal scale with different lags (0, 10, 20, 30, 40, and 50 years) over the past 114 and 800 years. Estimated temperatures are the average grid responses (multiple regression coefficients of standardized solar signals) on solar signals (21 year RMs) (supporting information). (a) Estimated temperature changes by solar variations [*Ball et al*., 2012; *Krivova et al*., 2010] over the past 114 years (1890–2003) using observed grid temperatures in 21 year RMs (GISS) [*Hansen et al*., 2010]. (b) Estimated temperature changes in proxy grid temperatures [*Mann et al*., 2009; *Morice et al*., 2012] due to solar variations [*Ball et al*., 2012; *Krivova et al*., 2010; *Steinhilber et al*., 2012] over the past 801 years in 21 year RM (1200–2000) (supporting information). To test the significance, 1000 autoregressive AR(1) models for solar signals were generated and regressed onto each grid temperature with the NH temperature as another variable. Only grids for which solar signals exceeded the AR(1) model results with 95% confidence (two tails) were plotted, and grids with 99% confidence were indicated by dots. The grey areas indicate the grids where continuous data are not available for the entire period. Note that we repeated the analyses with other data sets for observed global grid temperatures and solar signals and found similar spatiotemporal patterns in North Atlantic (Figure S6).

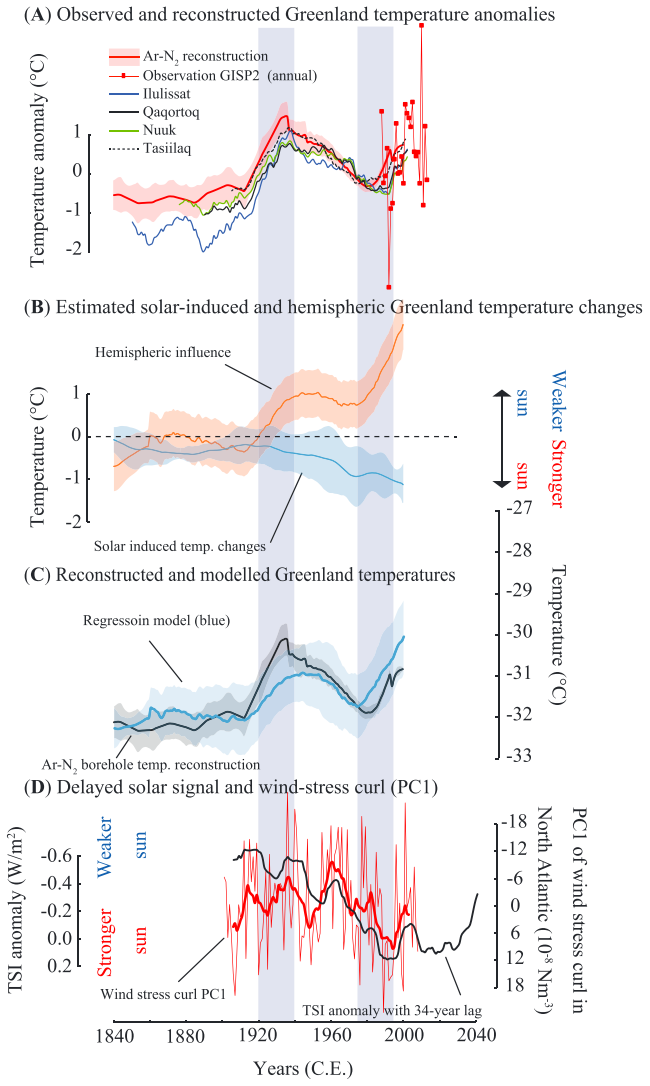

Figure 5. Greenland temperatures and climate indices during the observational period and future (1840–2040). (a) Observed and reconstructed Greenland temperature anomalies. Here temperature anomalies were relative to 1961–1990 averages of each time series. The thick red line is the reconstructed temperature from ice cores. The red rectangles connected with lines were observed annual average temperatures at GISP2 (1988–2013) [*Box*, 2013] after an adjustment for the mean to be the same as the reconstructed temperature anomalies for the overlapping period. Coastal temperatures in 21 year RMs are from Ilulissat (69°14′N, 51°4′W), Qaqortoq (60°43′N, 46°3′W), Nuuk (64°10′N, 51°42′W), and Tasiilaq (65°36′N, 37°38′W). (b) Decompositions of the Greenland temperatures as in Figure 3e but for 1840–2000. (c) Reconstructed and modeled Greenland temperatures as in Figure 3d but for 1840–2000. (d) Reconstructed TSI (black) in 11 year RMs [*Ball et al.*, 2012; *Krivova et al.*, 2010] anomaly (base year = 1961–1990) with 34 year lag (supporting information) from 1906 to 2041 and the first principal component (PC1; red) of the wind stress curl in the North Atlantic [*Häkkinen et al.*, 2011]. The thick and thin red lines indicate the PC1 of the wind stress curl [*Häkkinen et al.*, 2011] in the 11 year RMs and annual data for the periods from 1906 to 2003 and from 1901 to 2008, respectively. The two blue columns represent the periods (1920–1940 and 1975–1995) of positive and negative solar influences.

[*Chen and Tung*, 2014; *Gastineau and Frankignoul*, 2012; *Polyakov et al.*, 2010; *Rahmstorf et al.*, 2015], associated with a salinity anomaly in the North Atlantic [*Chen and Tung*, 2014; *Gastineau and Frankignoul*, 2012; *Polyakov et al.*, 2010]. Therefore, the lines of evidences indicate that the cold anomaly in Greenland and surrounding subpolar North Atlantic during the late twentieth century was primarily a result of solar-induced AMOC variability and associated atmospheric feedback processes, with a possible contribution from increasing greenhouse gas forcing [*Rahmstorf et al.*, 2015].

4. Discussions and Conclusions

Delayed responses in the subpolar North Atlantic and Greenland temperatures to solar variability suggest predictability on a multidecadal time scale. The modern solar maximum continued from the 1950s to the 1980s with an interruption in the 1970s. The 10 to 40 year lags (34 years based on the wind stress curl) suggest that the subpolar North Atlantic conditions temporally experience those conditions present in the 1990s and the effects (rapid warming) of the declining solar activity will become active decades later (Figure 5d). Given that solar activity is predicted to further decline over the next few decades [*Roth and Joos*, 2013], the subpolar North Atlantic may destabilize faster than projected for increasing greenhouse gases [*Collins et al.*, 2013], with the result of an intensified Greenland warming in the coming decades. If realized, this enhanced warming will impact predictions of sea level rise from Greenland ice and should be incorporated into the range of future model predictions. Finally, AMOC have been playing an important role on the transient distribution of the heat trapped by increasing greenhouse gases, inducing a global warming hiatus in the past decades [*Chen and Tung*, 2014; *Polyakov et al.*, 2010]. The proposed solar-induced AMOC variability provides a plausible explanation on the origin of the global warming hiatus.

Acknowledgments

This project was supported by KAKENHI (23710020, 25740007, and 22221002) and the EU Marie Curie Fellowship for T.K. The production of this paper was supported by an NIPR publication subsidy. This paper is dedicated to Thomas J. Crowley (1948–2014), who made substantial contributions to the field of paleoclimatology. We thank T. Stocker, H. Wanner, A. Born, S. Muthers, M. Döring, A. Jeltsch-Thömmes, H. Fischer, M. Leuenberger, and A. Ohmura for their comments and discussions. We also thank S. Häkkinen, R. Alley, J. Schwander, C. Buizert, A. Muto for the data, and K. Kawamura for hosting the experiments. We are also grateful to Sepp Kipfstuhl for the help in preparing the NGRIP ice samples. This paper was substantially improved by two anonymous reviews. T.K. conceived the project, conducted the analyses, and wrote the paper. J.B. and K.G.-A. contributed to the temperature reconstructions. B.M.V., T.B., and J.W. supported the interpretation of ice cores. T.N. and C.S.A. contributed on the climate data interpretations. All authors discussed the results, commented, and edited on the manuscript. This work is a contribution to the NorthGRIP ice core project, which is directed and organized by the Centre for Ice and Climate at the Niels Bohr Institute, University of Copenhagen. It is being supported by funding agencies in Denmark (SNF/FNU), Belgium (FNRS-CFB), France (IFRTP and INSU/CNRS), Germany (AWI), Iceland (Rannls), Japan (MEXT), Sweden (SPRS), Switzerland (SNF) and the United States of America (NSF).

The Editor thanks two anonymous reviewers for their assistance in evaluating this paper.

References

Ball, W. T., Y. C. Unruh, N. A. Krivova, S. Solanki, T. Wenzler, D. J. Mortlock, and A. H. Jaffe (2012), Reconstruction of total solar irradiance 1974–2009, *Astron. Astrophys.*, *541*, A27, doi:10.1051/0004-6361/201118702.

Box, J. E. (2013), Greenland Ice Sheet mass balance reconstruction. Part II: Surface mass balance (1840–2010), *J. Clim.*, *26*(18), 6974–6989.

Chen, X., and K.-K. Tung (2014), Varying planetary heat sink led to global-warming slowdown and acceleration, *Science*, *345*(6199), 897–903.

Collins, M., R. Knutti, J. Arblaster, J.-L. Dufresne, T. Fichefet, P. Friedlingstein, X. Gao, W. Gutowski, T. Johns, and G. Krinner (2013), Long-term climate change: Projections, commitments and irreversibility, in *Climate Change 2013: The Physical Science Basis. Contribution of Working Group I to the Fifth Assessment Report of the Intergovernmental Panel on Climate Change*, edited by T. F. Stocker et al., pp. 1029–1136, Cambridge Univ. Press, Cambridge, U. K.

Crowley, T. J. (2000), Causes of climate change over the past 1000 years, *Science*, *289*(5477), 270–277.

Cubasch, U., R. Voss, G. Hegerl, J. Waszkewitz, and T. Crowley (1997), Simulation of the influence of solar radiation variations on the global climate with an ocean-atmosphere general circulation model, *Clim. Dyn.*, *13*(11), 757–767.

Eichler, A., S. Olivier, K. Henderson, A. Laube, J. Beer, T. Papina, H. W. Gäggeler, and M. Schwikowski (2009), Temperature response in the Altai region lags solar forcing, *Geophys. Res. Lett.*, *36*, L01808, doi:10.1029/2008GL035930.

Gastineau, G., and C. Frankignoul (2012), Cold-season atmospheric response to the natural variability of the Atlantic Meridional Overturning Circulation, *Clim. Dyn.*, *39*(1–2), 37–57.

Goujon, C., J. M. Barnola, and C. Ritz (2003), Modeling the densification of polar firn including heat diffusion: Application to close-off characteristics and gas isotopic fractionation for Antarctica and Greenland sites, *J. Geophys. Res.*, *108*(D24), 4792, doi:10.1029/2002JD003319.

Gray, L., J. Beer, M. Geller, J. Haigh, M. Lockwood, K. Matthes, U. Cubasch, D. Fleitmann, G. Harrison, and L. Hood (2010), Solar influences on climate, *Rev. Geophys.*, *48*, RG4001, doi:10.1029/2009RG000282.

Häkkinen, S., P. B. Rhines, and D. L. Worthen (2011), Atmospheric blocking and Atlantic multidecadal ocean variability, *Science*, *334*(6056), 655–659.

Hanna, E., F. J. Navarro, F. Pattyn, C. M. Domingues, X. Fettweis, E. R. Ivins, R. J. Nicholls, C. Ritz, B. Smith, and S. Tulaczyk (2013), Ice-sheet mass balance and climate change, *Nature*, *498*(7452), 51–59.

Hansen, J., R. Ruedy, M. Sato, and K. Lo (2010), Global surface temperature change, *Rev. Geophys.*, *48*, RG4004, doi:10.1029/2010RG000345.

Hegerl, G. C., T. J. Crowley, M. Allen, W. T. Hyde, H. N. Pollack, J. Smerdon, and E. Zorita (2007), Detection of human influence on a new, validated 1500-year temperature reconstruction, *J. Clim.*, *20*(4), 650–666.

Kidston, J., A. A. Scaife, S. C. Hardiman, D. M. Mitchell, N. Butchart, M. P. Baldwin, and L. J. Gray (2015), Stratospheric influence on tropospheric jet streams, storm tracks and surface weather, *Nat. Geosci.*, *8*(6), 433–440, doi:10.1038/ngeo2424.

Kobashi, T., J. P. Severinghaus, J. M. Barnola, K. Kawamura, T. Carter, and T. Nakaegawa (2010), Persistent multi-decadal Greenland temperature fluctuation through the last millennium, *Clim. Change*, *100*, 733–756.

Kobashi, T., K. Kawamura, J. P. Severinghaus, J.-M. Barnola, T. Nakaegawa, B. M. Vinther, S. J. Johnsen, and J. E. Box (2011), High variability of Greenland surface temperature over the past 4000 years estimated from trapped air in an ice core, *Geophys. Res. Lett.*, *38*, L21501, doi:10.1029/2011GL049444.

Kobashi, T., K. Goto-Azuma, J. E. Box, C.-C. Gao, and T. Nakaegawa (2013a), Causes of Greenland temperature variability over the past 4000 years: Implications for Northern Hemispheric temperature change, *Clim. Past*, *9*, 2299–2317.

Kobashi, T., D. T. Shindell, K. Kodera, J. E. Box, T. Nakaegawa, and K. Kawamura (2013b), On the origin of Greenland temperature anomalies over the past 800 years, *Clim. Past*, *9*, 583–596.

Krivova, N. A., L. E. A. Vieira, and S. K. Solanki (2010), Reconstruction of solar spectral irradiance since the Maunder Minimum, *J. Geophys. Res.*, *115*, A12112, doi:10.1029/2010JA015431.

Levitus, S., J. I. Antonov, T. P. Boyer, O. K. Baranova, H. E. Garcia, R. A. Locarnini, A. V. Mishonov, J. Reagan, D. Seidov, and E. S. Yarosh (2012), World ocean heat content and thermosteric sea level change (0–2000 m), 1955–2010, *Geophys. Res. Lett.*, *39*, L10603, doi:10.1029/2012GL051106.

Ljungqvist, F. C. (2010), A new reconstruction of temperature variability in the extra-tropical Northern Hemisphere during the last two millennia, *Geogr. Ann. A*, *92*(3), 339–351.

Mann, M. E., Z. Zhang, M. K. Hughes, R. S. Bradley, S. K. Miller, S. Rutherford, and F. Ni (2008), Proxy-based reconstructions of hemispheric and global surface temperature variations over the past two millennia, *Proc. Natl. Acad. Sci. U.S.A.*, *105*, 13,252–13,257.

Mann, M. E., Z. Zhang, S. Rutherford, R. S. Bradley, M. K. Hughes, D. Shindell, C. Ammann, G. Faluvegi, and F. Ni (2009), Global signatures and dynamical origins of the Little Ice Age and Medieval Climate Anomaly, *Science*, *326*(5957), 1256–1260.

Menary, M., and A. Scaife (2014), Naturally forced multidecadal variability of the Atlantic Meridional Overturning Circulation, *Clim. Dyn.*, *42*(5–6), 1347–1362, doi:10.1007/s00382-013-2028-x.

Moberg, A., D. M. Sonechkin, K. Holmgren, N. M. Datsenko, and W. Karlen (2005), Highly variable Northern Hemisphere temperatures reconstructed from low- and high-resolution proxy data, *Nature*, *433*(7026), 613–617.

Morice, C. P., J. J. Kennedy, N. A. Rayner, and P. D. Jones (2012), Quantifying uncertainties in global and regional temperature change using an ensemble of observational estimates: The HadCRUT4 data set, *J. Geophys. Res.*, *117*, D08101, doi:10.1029/2011JD017187.

Polyakov, I. V., V. A. Alexeev, U. S. Bhatt, E. I. Polyakova, and X. Zhang (2010), North Atlantic warming: Patterns of long-term trend and multidecadal variability, *Clim. Dyn.*, *34*(2–3), 439–457.

Rahmstorf, S., J. E. Box, G. Feulner, M. E. Mann, A. Robinson, S. Rutherford, and E. J. Schaffernicht (2015), Exceptional twentieth-century slowdown in Atlantic Ocean overturning circulation, *Nat. Clim. Change*, *5*(5), 475–480, doi:10.1038/nclimate2554.

Roth, R., and F. Joos (2013), A reconstruction of radiocarbon production and total solar irradiance from the Holocene ^{14}C and CO_2 records: Implications of data and model uncertainties, *Clim. Past*, *9*(4), 1879–1909, doi:10.5194/cp-9-1879-2013.

Scaife, A. A., S. Ineson, J. R. Knight, L. Gray, K. Kodera, and D. M. Smith (2013), A mechanism for lagged North Atlantic climate response to solar variability, *Geophys. Res. Lett.*, *40*, 434–439, doi:10.1002/grl.50099.

Severinghaus, J. P., T. Sowers, E. J. Brook, R. B. Alley, and M. L. Bender (1998), Timing of abrupt climate change at the end of the Younger Dryas interval from thermally fractionated gases in polar ice, *Nature*, *391*(6663), 141–146.

Shindell, D. T., G. A. Schmidt, M. E. Mann, D. Rind, and A. Waple (2001), Solar forcing of regional climate change during the Maunder Minimum, *Science*, *294*(5549), 2149–2152.

Steinhilber, F., J. A. Abreu, J. Beer, I. Brunner, M. Christl, H. Fischer, U. Heikkilä, P. W. Kubik, M. Mann, and K. G. McCracken (2012), 9,400 years of cosmic radiation and solar activity from ice cores and tree rings, *Proc. Natl. Acad. Sci. U.S.A.*, *109*(16), 5967–5971.

Swingedouw, D., L. Terray, C. Cassou, A. Voldoire, D. Salas-Mélia, and J. Servonnat (2011), Natural forcing of climate during the last millennium: Fingerprint of solar variability, *Clim. Dyn.*, *36*(7), 1349–1364.

Waple, A., M. Mann, and R. Bradley (2002), Long-term patterns of solar irradiance forcing in model experiments and proxy based surface temperature reconstructions, *Clim. Dyn.*, *18*(7), 563–578.